

SINGLE STEP SYNTHESIS OF MAGNESIUM FERRITE NANOCRYSTALLITES AND SOME OF ITS CHARACTERISTICS

AYE AYE THANT^{*,§,||}, SRIMALA SREEKANTAN^{*}, PHO KAUNG[†],
MITSURU ITOH[‡], RADZALI OTHMAN^{*} and M. N. AHMAD FAUZI^{*,¶,||}

^{*}*School of Materials and Mineral Resources Engineering
Universiti Sains Malaysia, Engineering Campus
14300, Nibong Tebal, Pulau Pinang, Malaysia*

[†]*Physics Department, University of Yangon, Kamayut, Yangon, Myanmar*

[‡]*Materials and Structures Laboratory, Tokyo Institute of Technology, 4259
Nagatsuta, Midori, Yokohama 226-8503, Japan*

[§]*a2thant@gmail.com*

[¶]*afauzi@eng.usm.my*

The present study elucidates the synthesis of magnesium ferrite magnetic nanocrystallites via hydroxylation–condensation reaction followed by an auto-combustion process. Nanocrystallites with diameter of 3–7 nm were successfully formed via this method. The ignition temperature of the redox reaction was apparently improved to 200°C by the modification of the pH of the metal aqueous solution. The crystallite size was altered by varying the hydrolysis parameters. The XRD analysis of the as-synthesized powder confirms the formation of a single-phase MgFe₂O₄ spinel structure. Importantly, the crystalline particles were obtained at low temperature without further calcination. The thermodynamic behavior of the precursor was characterized by DTA-TG. TEM observations showed the morphology and crystal structure of the nanocrystallites.

Keywords: MgFe₂O₄; nanocrystallite; sol–gel; auto-combustion; synthesis.

1. Introduction

Auto-combustion assisted sol–gel synthesis (SGAC) is a promising method to produce nanocrystalline ceramic powder as it can produce nanosized powder at relatively low temperature with high homogeneity for better sinterability. In SGAC, thermally induced anionic redox reaction involves the nitrate ions of the metal precursor as oxidizer and citric acid as a fuel providing the energy for the formation of oxide within a short time.^{1,2} It offers many advantages compared with other routes such as low

cost, excellent compositional control, good powder reactivity, and >99.9% purity.³ Spinel ferrites in general and magnesium ferrite in particular are technologically important materials and have found widespread application in microwave devices.⁴ Low-temperature ferrite can improve the electrical and magnetic properties.⁵

Huang *et al.*⁶ prepared MgFe₂O₄ nanocrystallites through sol–gel auto-combustion method. The decomposition of ferrite precursor occurred at 340°C without pH modification. Pradeep *et al.*^{7,8}

^{||}Corresponding authors.

and Rezlescu *et al.*⁹ also prepared pure and substituted MgFe_2O_4 by sol-gel auto-combustion method.

However, the modification of pH and the hydrolysis conditions on the synthesized powder were not reported. Hence, an attempt has been made to investigate the influence of pH modification and hydrolysis conditions on the combustion characteristic and the morphology of the MgFe_2O_4 powder synthesized by low-temperature sol-gel auto-combustion method.

2. Experimental Procedure

The flowchart for the synthesis procedure is shown in Fig. 1. The starting materials were analytical reagent grade nitrates: $\text{Fe}(\text{NO}_3)_3 \cdot 9\text{H}_2\text{O}$ (Wako 99.0%), $\text{Mg}(\text{NO}_3)_2 \cdot 6\text{H}_2\text{O}$ (Wako 98.0%), and citric acid (Wako 98.0%). The molar ratio of metal nitrate to citric acid was 1:1. Ammonia solution (NH_4 28%) was added dropwise under constant stirring to reach the pH value to 9. Then, the solution was evaporated on a hot plate at a solution temperature 60°C to form a sticky gel. The temperature of the hydrolysis was varied 60, 70, and 80°C in order to investigate the effect of hydrolysis temperature on the form of MgFe_2O_4 . Upon the formation of a dense sticky gel, the temperature was increased to 80°C for the condensation process. The temperature was then increased rapidly and when it reached to $\sim 200^\circ\text{C}$, large amount of gases (CO_2 , H_2O , N_2) were liberated and a dark brown ferrite powder was produced after the combustion process.

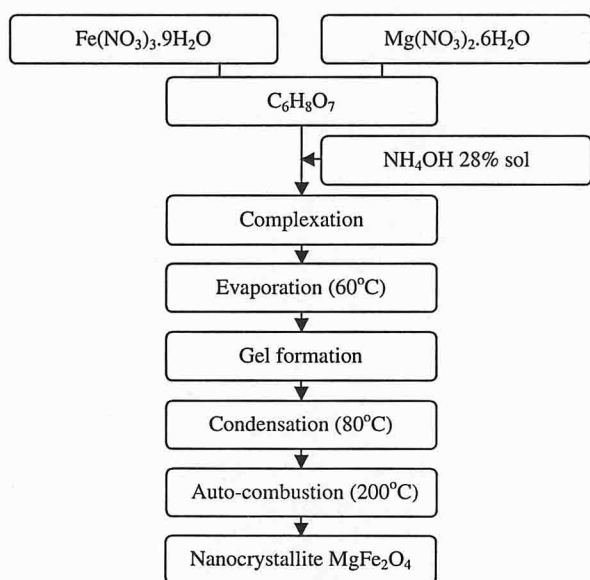


Fig. 1. Flowchart for one-step synthesis of MgFe_2O_4 .

The X-ray diffraction patterns were recorded on an SRA (M18XHF) X-ray diffractometer. Transmission Electron Microscopy was acquired by JEOL JEM2010F. The thermal behavior of the dried gel precursors were characterized by TG-DTA 2000S (Japan) at a heating rate of $10^\circ\text{C}/\text{min}$ until 500°C under O_2 flow at $100\text{ ml}/\text{min}$.

3. Results and Discussion

3.1. X-Ray analysis

The XRD spectrums of the precursor and the powder heat-treated at 1000°C are shown in Fig. 2. The precursor of the original solution with $\text{pH} < 1$ in (B) is amorphous in nature while the precursor with $\text{pH} = 9$ in (A) shows amorphous MgFe_2O_4 with crystallized NH_4NO_3 phase indicating NH_4NO_3 was crystallized during hydrolysis as NH_4 solution was used to reach the pH value to 9. The precursors were then heat-treated at 1000°C to observe the stability of the phase. Both spectrums in (C) and (D) show the formation of single-phase ferrite (PDF 01-071-1232). The lattice parameter and the crystallite size estimated by the Debye-Scherrer formula¹⁰ are shown in Table 1.

The crystallite size decreased with the increased in pH value showing that the presence of ammonia during the hydrolysis can affect the size of the particle.

Figure 3 represents the formation of MgFe_2O_4 at various hydrolysis temperatures at $\text{pH} = 9$. The results demonstrate that the degree of crystallinity

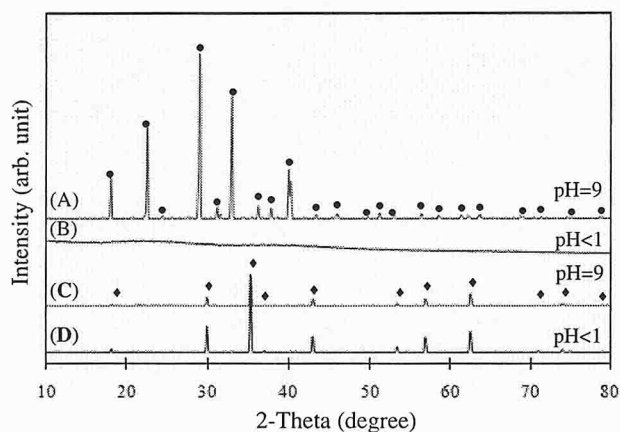


Fig. 2. XRD spectrums of (A) amorphous MgFe_2O_4 with crystallized NH_4NO_3 ($\bullet = \text{NH}_4\text{NO}_3$) at $\text{pH} = 9$, (B) amorphous MgFe_2O_4 at $\text{pH} < 1$, and crystallized MgFe_2O_4 heat-treated at 1000°C (C) at $\text{pH} = 9$, (D) at $\text{pH} < 1$ ($\blacklozenge = \text{MgFe}_2\text{O}_4$).

Table 1. Lattice parameter and crystallite size calculated from XRD data (after heat-treated at 1000°C).

Sample	Crystallite size (nm)	Lattice parameter (Å)
pH < 1	36.84	8.3879
pH = 9.00	29.48	8.3860

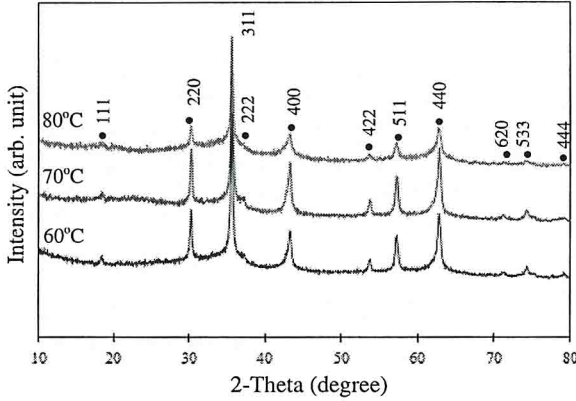


Fig. 3. XRD spectrums of as-burnt powder (pH = 9) at different hydrolysis temperatures (● = MgFe₂O₄).

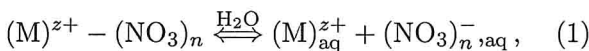
can be altered by varying the hydrolysis temperature. As the hydrolysis temperature was increased, the duration to form gel becomes shorter and that favors the formation of small crystallite size. This is confirmed by the TEM images and auto-combustion behavior in the following sections.

3.2. TEM analysis

From TEM analysis, the crystallite size of the powder (60°C hydrolysis) is ~7 nm and that of the powder (80°C hydrolysis) is ~3 nm as shown in Fig. 4. As shown the as-burnt powder, the shape of the particle was irregular and the particles seem to be composed of crystallites. It exhibits a soft agglomerated monophasic polycrystal with the particles holding together by a relatively weak secondary bond of magnetic interaction.¹¹

3.3. TG-DTA characterization

In aqueous chemistry,¹² water plays a double role. It behaves as a solvent with a high dielectric constant ($\epsilon = 80$) that favors the dissociation of ionic species as



where M is metal ion. It also behaves as a σ -donor molecule and reacts as a nucleophilic ligand giving

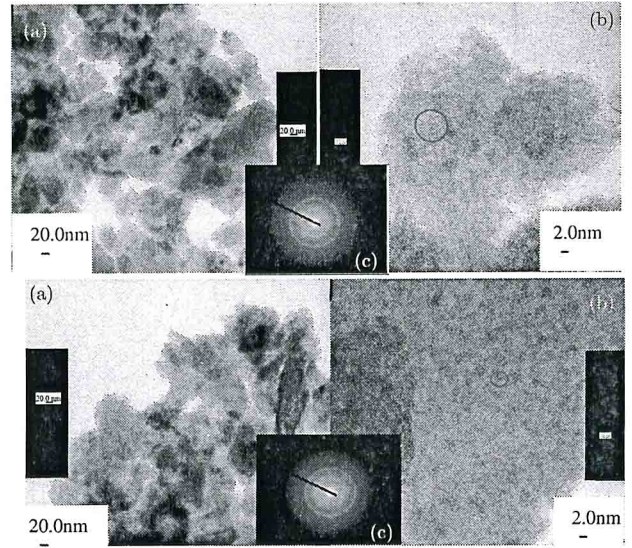
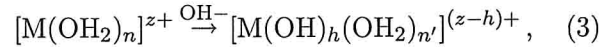


Fig. 4. TEM (a) low resolution, (b) high resolution, and (c) corresponding ED images of the as-burnt powder at hydrolysis temperature 60°C (above) and 80°C (below).

solvated species as

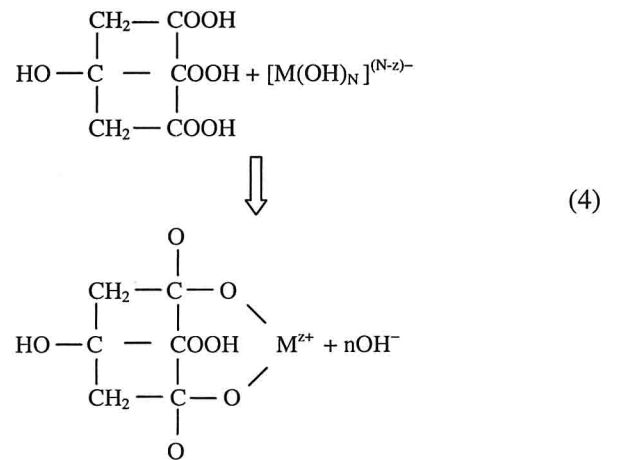


When the pH increases,

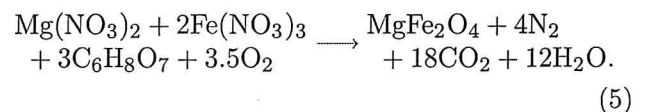


where h is the hydrolysis ratio.

Citric acid also plays a double role: as a fuel for combustion reaction and as a chelating agent to form complexes with metal ions as



On these basics, we have proposed a chemical reaction as



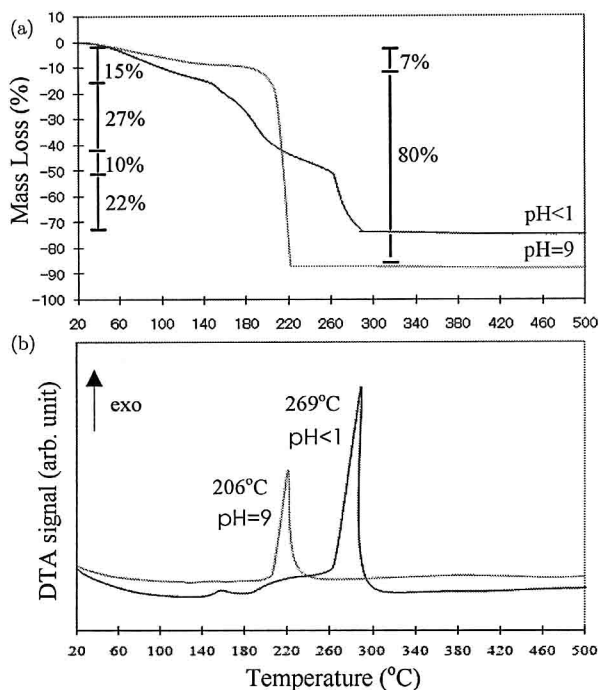


Fig. 5. (a) TG and (b) DTA plots of the precursors.

It is worth to note that the thermal decomposition of the precursor with $\text{pH} < 1$ consists of four steps, while the other with $\text{pH} = 9$ shows only two steps as shown in Figs. 5(a) and 5(b). According to partial charge model, the intermediate pH region having aquo, $[\text{M}(\text{OH}_2)_N]^{z+}$, and hydroxo, $[\text{M}(\text{OH})_N]^{(N-z)-}$, ligands have better condensation process than the low pH region having aquo, $[\text{M}(\text{OH}_2)_N]^{z+}$, ligand.¹³ On that basis, one point that improved the weight loss in pH modified gel may be due to the different condensation process between the pH modified aqueous solution and the original aqueous solution. In fact, O–H groups, carboxyl group, and NO_3^- ions exist in the dried gel.¹⁴ In the TG-DTA curve of the dried gel ($\text{pH} < 1$), the first weight loss (15%) represents the water vaporization of O–H groups, the second weight loss (27%) corresponds with the decomposition of citric acid to aconitic acid $\text{C}_6\text{H}_6\text{O}_6$ ($-\text{H}_2\text{O}$) and then decomposed to itaconic acid $\text{C}_5\text{H}_6\text{O}_4$ ($-\text{CO}_2$) in the third weight loss (10%). It was confirmed by the DTA plot of the solid citric acid. Finally carboxyl groups and NO_3^- ions decomposed leading to the auto-combustion reaction in the fourth step (22%). However, in the dried gel with $\text{pH} = 9$, the weight loss (7%) for vaporization reduced slightly in the first step. In the second step, a deep weight loss (80%) represents the decomposition of

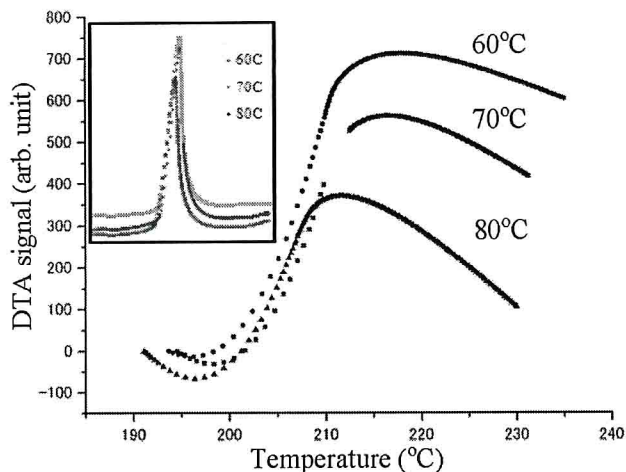


Fig. 6. The DTA curves for different hydrolysis temperatures and respective integral curves in the insect at $\text{pH} = 9$.

carboxyl, NO_3^- ions and NH_4NO_3 simultaneously and auto-combustion occurred. The decomposition of NH_4NO_3 supplies oxygen to accelerate the combustion reaction. Not only the combustion temperature was decreased but also the amount of heat generated in the combustion process was also apparently decreased as shown in Fig. 6. It proved that the decomposition of NH_4NO_3 was an endothermic process. Thus, it resulted in reduced amount of heat generated during the combustion process and produces small crystallite size.

Therefore, it is confirmed that the amount of heat produced depends on the hydrolysis temperature and time, which is a key factor affecting the size and morphology of the particles.

4. Conclusion

The auto-combustion assisted sol-gel method has been proven as a low-temperature synthesis route for homogeneous powder with fine particles. Not only the decomposition temperature of the nitrate-citrate was apparently improved to 200°C , but also the amount of heat generated during the combustion was also reduced by pH modification of the aqueous solution. Furthermore, the hydrolysis conditions can affect the combustion behavior and govern the crystallite size. Better understanding on the decomposition of citrate-nitrate precursor has been established in this study.

Acknowledgment

The authors are grateful to ASEAN University Network/Southeast Asia Engineering Education

Development Network (AUN/SEED-Net) for the financial support.

References

1. P. K. Roy and J. Bera, *J. Mater. Proc. Tech.* **197**, 279 (2008).
2. K. H. Wu, T. H. Ting, M. C. Lia and W. D. Ho, *J. Magn. Magn. Mater.* **298**, 25 (2006).
3. W. J. Dawson, *Ceramic Bull.* **67**, 1673 (1988).
4. A. Dogra, M. Singh and R. Kuma, *Nucl. Instr. Meth. B* **207**, 296 (2003).
5. L. Zhao, H. Yang, L. Yu, Y. Cui, X. Zhao, B. Zou and S. Feng, *J. Magn. Magn. Mater.* **301**, 445 (2006).
6. Y. Huang, Y. Tang, J. Wang and Q. Chen, *Mater. Chem. Phys.* **97**, 394 (2008).
7. A. Pradeep, P. Priyadharsini and G. Chandrasekaran, *Mater. Chem. Phys.* **320**, 2774 (2008).
8. A. Pradeep and G. Chandrasekaran, *Mater. Lett.* **60**, 371 (2006).
9. N. Rezlescu, C. Doroftei and P. D. Popa, *Rom. J. Phys.* **52**, 353 (2007).
10. B. E. Warren and B. L. Averbach, *J. Appl. Phys.* **21**, 595 (1950).
11. W. E. Lee and W. M. Rainforth, *Ceramic Microstructure* (Chapman & Hall, 1994).
12. J. Livage, C. Sanchez, M. Henry and S. Doeuff, *Solid State Ionics* **32/33**, 633 (1989).
13. C. J. Brinker and G. W. Scherer, *Sol-Gel Science* (Academic Press, San Diego, 1990).
14. M. Epifani, E. Melissano, G. Pace and M. Schioppa, *J. Eur. Ceram. Soc.* **27**, 115 (2007).